An Experimental Study on Pounding Force between Reinforced Concrete Slabs

Sushil Khatiwada[1], Nawawi Chouw[2] and Tam Larkin[3]

1. Corresponding Author. PhD Candidate, Department of Civil and Environmental Engineering, The University of Auckland, Auckland 1023.
   Email: skha178@aucklanduni.ac.nz

2. Associate Professor, Department of Civil and Environmental Engineering, The University of Auckland, Auckland 1023. Email: n.chouw@auckland.ac.nz

3. Senior Lecturer, Department of Civil and Environmental Engineering, The University of Auckland, Auckland 1023. Email: t.larkin@auckland.ac.nz

Abstract

Building pounding, defined as the earthquake induced collision between insufficiently spaced buildings, has been recognized as a recurring urban seismic hazard. Numerous studies have been carried out in the past decades on the severity of the hazard. Most of the studies employ a contact force approach, where an elastic or viscoelastic link is placed between the colliding masses in series with a gap. The link is activated when the gap is closed and the pounding force is calculated from the deformation, and rate of change of deformation of this link. Several numerical models have been proposed to compute the pounding force. Past studies have compared the performance of these models in predicting force due to the impact of a sphere falling on a floor or a beam. However, building pounding is the collision of distributed masses i.e. slabs or beams of structures and few such experimental results exist. This study presents the force due to the pounding of two suspended reinforced concrete slabs. The effects of variation in velocity are shown. The experimental results were compared with the predictions of numerical models. The results show that the updated Hertzdamp model had the least error in the prediction of pounding force.

Keywords: building pounding, pounding force, concrete slabs impact, impact element method

1 INTRODUCTION

Past major urban earthquakes have shown that buildings can collide and damage each other (Rosenblueth and Meli 1986) if there is insufficient separation to accommodate the relative movement. This type of collision, termed pounding, has also been observed when two bridge decks collide or a bridge deck collides with the abutment (Malhotra 1998; Chouw and Hao

2008; Li *et al.* 2013). The relative motion is due to the out-of-phase vibration of adjacent buildings. The phase difference can be induced by differing structural properties (Anagnostopoulos 1988), differing foundation soil (Schmid and Chouw 1992; Chouw 2002) or due to the spatial variation of ground motion (Li *et al.* 2012). Cole *et al*. (2012) documented many instances of pounding observed in the Christchurch 2011 earthquake, which produced very minor, aesthetic damage as well as major structural damage in buildings. Chouw and Hao (2012) presented many instances of building and bridge pounding in the same earthquake as well as several instances of vertical pounding.

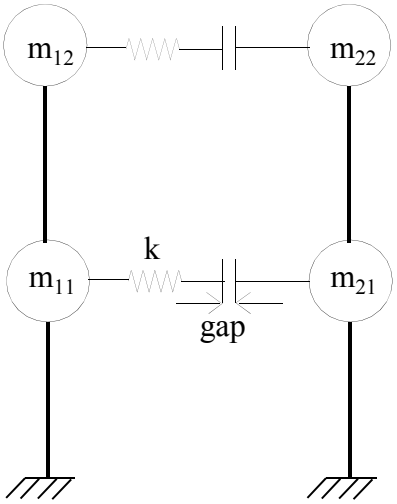

Fig. 1. Lumped mass model of pounding.

Seismic pounding has been simulated as either the collision of masses concentrated at a point *i.e*. a lumped mass model or as impact between distributed masses. In the lumped mass model (Fig. 1), the floor masses of the structures are lumped at a level, and the structures are idealized as single degree-of-freedom (SDoF) or multiple degrees-of-freedom (MDoF) according to the number of storeys (Anagnostopoulos 1988). It is assumed that the response of the structure can be calculated as if the pounding force is concentrated on the centre of mass of the colliding floors. In the distributed mass model (Fig. 2), the floor mass is distributed over its length. The force acts on the contact surface and its effects take time to distribute throughout the length. Most distributed mass models are derived or validated with the Saint-Venant's theory of impact, also known as wave propagation theory (Malhotra 1998; Cole *et al.* 2010).

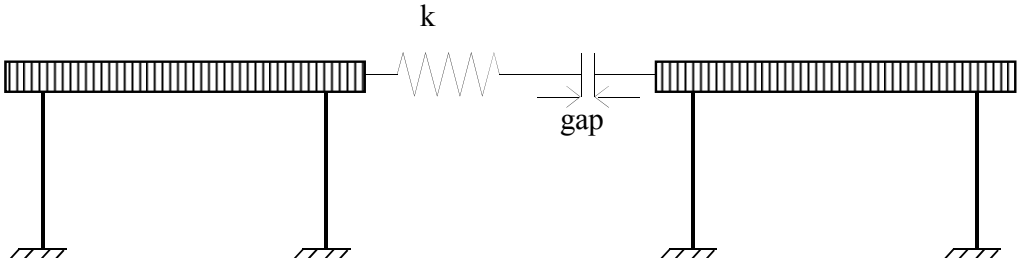

Fig. 2. Distributed mass model.

Several numerical force models have been proposed for both these methods. A detailed treatment of the lumped mass models have been provided in Khatiwada *et al.* (2013a) while Khatiwada *et al.* (2013b) discussed distributed mass models in more detail. The discussions

have not been reproduced here due to page limitations. Khatiwada *et al.* (2013a) attempted to identify the best performing lumped mass model from the shake table investigation of pounding between steel portal frames. Several pairs of frames were subjected to pounding under five different ground motions and the amplification of maximum displacement of the beams was calculated for each case. The simulations were repeated numerically with five different numerical force models. It was observed that all the numerical models predicted similar amplification ratios. Thus the models were found to be equally correct under some ground motions and equally incorrect under others. It was postulated that the high error under more severe ground motions could be due to velocity dependence of the coefficient of restitution which is a measure of energy loss during each impact. Khatiwada and Chouw (2013) considered the consequence of pounding for buildings in a row.

This study is a continuation of the effort to identify the best performing numerical force model for analysis of pounding. Two reinforced concrete (RC) slabs were suspended from an overhead support and subjected to impact. The acceleration and displacement of the slabs were measured. The pounding force and coefficient of restitution were calculated. The force was also simulated from five different models and compared with the pounding force from the experiments to identify the best performing model.

2 NUMERICAL FORCE MODELS

Five viscoelastic force models, defined for lumped mass idealization, were included in the study. The models are defined for two bodies of mass m_1 and m_2, connected by a spring and a dashpot which are arranged in series with a 'gap' that is equal to the separation gap between the structures (Fig. 3). At any time t, the displacement of the bodies is u_1 and u_2 and velocities are v_1 and v_2. If u_1 - u_2 is greater than the gap, the bodies are in contact and pounding force exists otherwise the force is zero. All models calculate pounding force F as a function of relative deformation $\delta = u_1 - u_2$, and relative velocity $\dot{\delta} = v_1 - v_2$. The viscous energy loss depends upon a predetermined coefficient of restitution e.

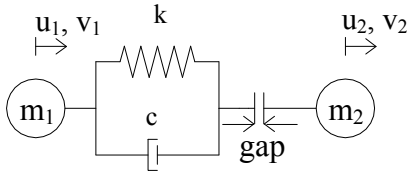

Fig. 3. Viscoelastic model of lumped mass impact.

The detailed descriptions of the models can be found in comparative studies by Jankowski (2005), Muthukumar and DesRoches (2006) and Khatiwada *et al.* (2013a).

2.1 Linear viscoelastic model (LVe)

$$F = k\,\delta + c\,\dot{\delta} \tag{1}$$

where, c is the damping constant given by,

$$c = 2\,\xi\sqrt{k\,\frac{m_1\,m_2}{m_1 + m_2}} \tag{2}$$

and damping ratio ξ can be obtained from:

$$\xi = \frac{-\ln(e)}{\sqrt{\pi^2 + \ln(e)^2}} \tag{3}$$

2.2 Modified linear viscoelastic model (MLVe)

$$\begin{aligned} F &= k\delta + c\dot{\delta}; & \dot{\delta} \geq 0 \\ F &= k\delta; & \dot{\delta} < 0 \end{aligned} \tag{4}$$

where the approach only damping constant, *c*, can be calculated from Equation (3) but the expression of damping ratio ξ is modified to

$$\xi = \frac{1}{\pi}\frac{1-e^2}{e} \tag{5}$$

2.3 Nonlinear viscoelastic model (NlVe)

$$\begin{aligned} F &= k\delta^{3/2} + \bar{c}\dot{\delta}\ ; & \dot{\delta} \geq 0 \\ F &= k\delta^{3/2}\ ; & \dot{\delta} < 0 \end{aligned} \tag{6}$$

where instantaneous damping $\bar{c}$ is given by:

$$\bar{c} = 2\bar{\xi}\sqrt{k\sqrt{\delta}\frac{m_1 m_2}{m_1 + m_2}}$$

and $\bar{\xi} = \frac{9\sqrt{5}}{2}\frac{1-e^2}{e(e(9\pi-16)+16)}$

2.4 Updated Hertzdamp model (Hd)

$$F = k\delta^{3/2} + \zeta\delta^{3/2}\dot{\delta} \tag{7}$$

where the viscoelastic part of the force depends upon the relative deformation and relative velocity. The damping factor ζ is obtained from the implicit equation,

$$(1+e) = \frac{k}{\zeta\dot{\delta}_0}\ln\left|\frac{\frac{k}{\zeta\dot{\delta}_0}+1}{\frac{k}{\zeta\dot{\delta}_0}-e}\right| \tag{8}$$

2.5 Linear Hunt-Crossley model (LHC)

$$F = k\delta + \zeta\,\delta\,\dot{\delta} \tag{9}$$

where the damping factor ζ is same as that for Hd model (Equation (8))

The LVE, MLVe and NlVe models were respectively proposed by Anagnostopoulos (1988), Mahmoud (2008) and Jankowski (2005). The last two models (Hd and LHC) were obtained by the current authors (unpublished) while attempting to correct the error in Hertzdamp (Muthukumar and DesRoches 2006) and modified Hertzdamp (Ye *et al.* 2009b) models. The two equations are linear and nonlinear form of the Hunt-Crossley model (Zhang and Sharf 2009). Equation (8) is the numerically exact solution of the Hunt-Crossley models which had

been approximately solved previously as Hertzdamp, modified Hertzdamp and modified Kelvin impact model (Ye *et al.* 2009a)

3 EXPERIMENTAL SETUP

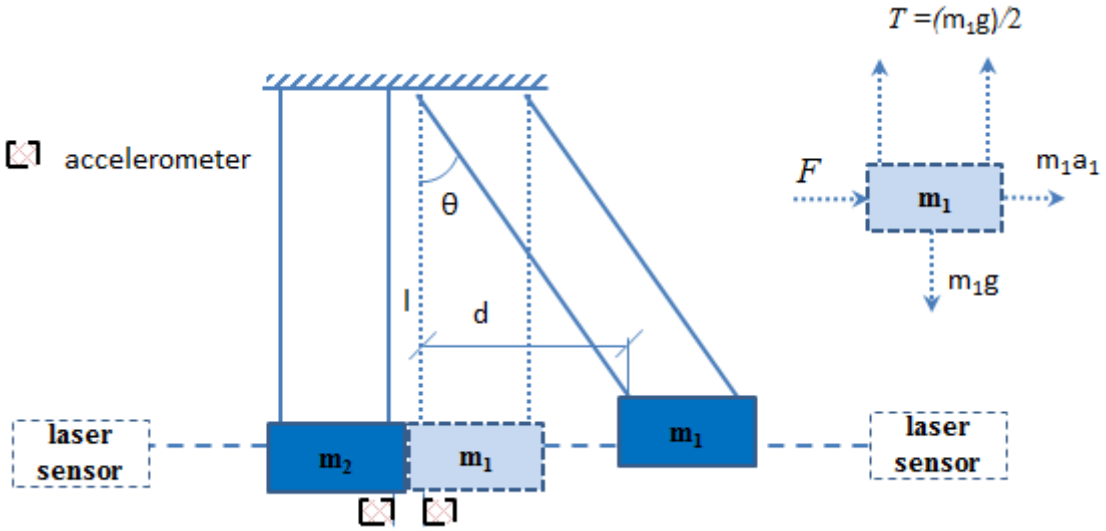

Fig. 4. Schematic of the experimental setup.

The experiment was set up as forcing an impact between two pendulums (Fig. 4). The RC slabs of size 550 x 550 x 120 mm were hung from overhead support, with four cables each. The length of the cables was 1.5 m. Initially, the slabs were just touching each other. The impact was induced by pulling one of the slabs, termed striker, to a certain distance and releasing it so that it hit the second slab just as it reached the lowermost point in its displacement path. A laser sensor was used to measure the displacement of the far end of each slab while two accelerometers were used to record the acceleration during impact. During the test, the initial displacement was measured approximately. During calculation, the actual initial and final displacements were obtained from the lasers. The dynamic equilibrium of the striker is shown in the upper right corner of Fig. 4. Thus, the pounding force can be calculated as a product of mass and acceleration of the striker.

Fig. 5. Photograph of the test setup.

At the contact end, a detachable pounding element was bolted to each slab, to save the main body from impact damage at the contact surface. Both pounding elements had a dimension of 100 x 550 x 120 mm but the striker had a hemispherical protrusion of 100 mm diameter at its center (Fig. 5). Thus, the pounding force was assumed to be concentrated at the center of the

contact ends. The slabs had a mass of 95 kg each, the striker's attachment was 15 kg and the struck slab's attachment was 14 kg.

Eight tests were carried out for d = 10, 15, 37, 56, 66, 71, 87 and 94 mm. The data was recorded at 10 kHz sampling rate. Perhaps due to the low impact velocities, no damage was observed at the pounding locations after the tests.

4 RESULTS AND DISCUSSIONS

The pounding forces obtained at two different impact velocities are shown in Fig. 6. The negative part of the force was quite surprising. After negative forces were observed, the test setup was re-checked thoroughly for the presence of any deficiencies. A few of the impacts were repeated a number of times and a video recording was made, which was reviewed thoroughly for the presence of any out-of-plane movement or other errors. It was observed that the results were always as shown in Fig. 6 with both negative and positive oscillations. The video recordings showed no significant out-of-plane movement for the first two impacts in each test though there was some out-of-plane movement after the third or fourth impact in each test. Finally, it was assumed that the oscillations were due to the internal vibrations of the slabs due to impact. Thus, for the evaluation of lumped mass models, only the first positive pulse of force has been considered.

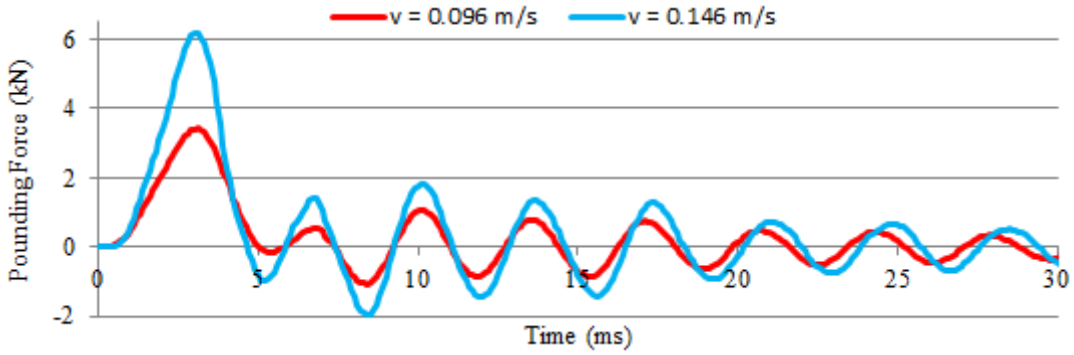

Fig. 6. Pounding force recorded from two impacts

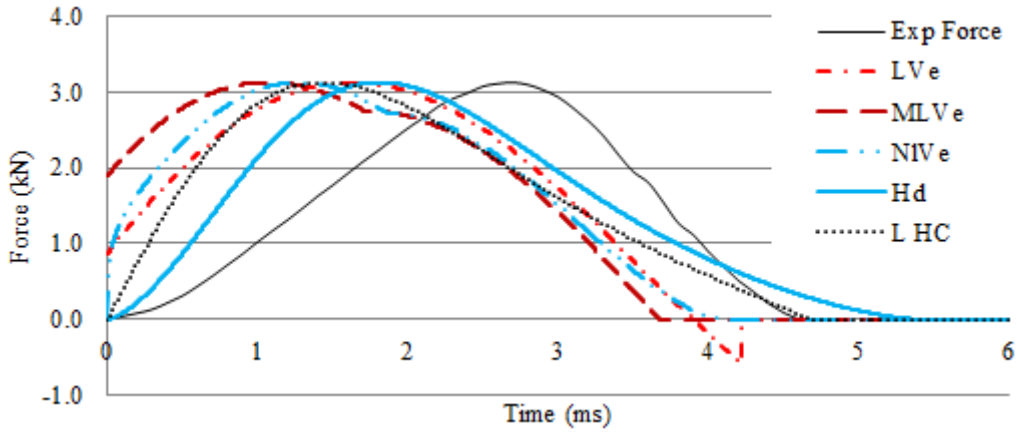

Fig. 7. Simulated and measured pounding force for impact velocity 0.096 m/s

The final velocities of the slabs were calculated from the post-impact displacements and the coefficient of restitution for each impact was calculated as the ratio of relative velocities after

and before impact. For the two velocities shown in Fig. 6, the coefficient of restitution was approximately 0.7.

For each impact test, numerical simulations were carried out with the five numerical models described in Section 2. A time step of 10 μs was adopted in the calculations. For each impact, the stiffness *k* for each model was optimized so that the peak simulated force was equal to the peak experimental force. Fig. 7 shows the simulated and measured force for an impact velocity 0.096 m/s.

Table 1 shows the normalized error (NE) in predictions for the models as defined in Equation (10). It is apparent that Hd model has the least error in all the cases, sometimes almost half of the other models. Although the LHC model is defined for linear stiffness, it performed better than the NlVe model which is based on Hertz contact law for curved surfaces even though the contact surface was spherical. The LVe model proved to be as accurate as NlVe even though it was not derived for the prediction of pounding forces. The MLVE model always has the highest normalized error.

$$\mathrm{NE} = \frac{\sqrt{\sum_{i=1}^{n}(F_m - F_r)^2}}{\sqrt{\sum_{i=1}^{n}(F_r)^2}} \tag{10}$$

where n is the total number of time-steps, F_m is the force predicted at i^{th} time-step by the model and F_r is the force recorded in the experiment at the same time-step.

Table 1. Normalized error in simulated forces

Trial	Velocity (m/s)	Normalized Error NE				
		LVe	MLVe	NlVe	Hd	LHC
1	0.030	50.18%	69.53%	61.42%	26.12%	43.38%
2	0.040	74.25%	87.32%	79.59%	48.14%	64.52%
3	0.096	62.33%	79.14%	68.39%	38.81%	56.68%
4	0.146	80.22%	94.44%	83.04%	56.66%	73.60%
5	0.171	91.76%	103.11%	92.08%	69.06%	84.97%
6	0.183	79.89%	91.55%	76.87%	57.92%	76.31%
7	0.226	90.22%	101.03%	91.24%	67.36%	82.65%
8	0.243	81.93%	93.15%	81.04%	60.30%	76.92%

It can be observed from Table 1 that the predictions from all five numerical models are closer to each other than to the experimental results. For instance: the NE for Hd model in Trial 5 is 56% while the average error of all five models is 77.59%. Similarly, the rising curve of simulated force (Fig. 7) is steeper than the falling curve and the force time-history is right-skewed but the experimental force shows opposite characteristics. "Finally, the oscillations observed in the force time-histories (Fig. 6) suggests that even these relatively short slabs showed the effects of internal vibrations of distributed mass. Thus, the applicability of lumped mass models to simulate pounding between considerably longer building slabs or bridge decks needs to be reassessed, for example, with larger scale impact tests. The wave propagation effects cannot be isolated in these slabs because the first fundamental period of internal vibration is 0.4 ms, while the first positive pulse of acceleration is ten times that.

5 CONCLUSIONS

Two RC slabs were arranged to impact against each other at different impact velocities. The contact surface is spherical on one slab and planar on the other. The pounding forces were calculated from the impact accelerations according to Newton's second law of motion, while the coefficient of restitution for each impact was calculated from the post-impact maximum displacement of the slabs. The impact forces were also simulated with five numerical models for each impact velocity with the coefficient of restitution calculated from the experimental data. The normalized error of simulation was also calculated and shows that the updated Hertzdamp model had the least simulation errors while the modified viscoelastic model had the largest errors for all impacts.

Further large scale impact tests are required to verify the results. The large scale tests will also be able to identify the presence of distributed mass effects, suggested by these tests, more accurately.

ACKNOWLEDGEMENT:

The authors would like to thank the University of Auckland for the first author's doctoral scholarship.

REFERENCES:

Anagnostopoulos, S.A. (1988) Pounding of buildings in series during earthquakes, Earthquake Eng Struct Dyn Vol 16, No 3, pp 443-56.

Chouw, N. (2002) Influence of soil-structure interaction on pounding response of adjacent buildings due to near-source earthquakes, JSCE J Appl Mech Vol 5, pp 543-53.

Chouw, N. and Hao, H. (2008) Significance of ssi and nonuniform near-fault ground motions in bridge response I: Effect on response with conventional expansion joint, Eng Struct Vol 30, No 1, pp 141-53.

Chouw, N. and Hao, H. (2012) Pounding damage to buildings and bridges in the 22 february 2011 christchurch earthquake, Int J of Protective Struct Vol 3, No 2, pp 123-40.

Cole, G.L., Dhakal, R.P., Carr, A. and Bull, D. (2010) An investigation of the effects of mass distribution on pounding structures, Earthquake Eng Struct Dyn Vol 40, No 6, pp 641-59.

Jankowski, R. (2005) Non linear viscoelastic modelling of earthquake induced structural pounding, Earthquake Eng Struct Dyn Vol 34, No 6, pp 595-611.

Khatiwada, S., Chouw, N. and Butterworth, J. (2013a). Evaluation of numerical pounding models with experimental validation, NZSEE Bulletin Vol 46, No 3, pp 117-30. .

Khatiwada, S., Chouw, N. and Larkin, T. (2013b). Simulation of structural pounding with the sears impact model, 4th Conf on Comp Meth in Struct Dyn and Earthq Eng, Kos, Greece.

Khatiwada, S. and Chouw, N. (2013) A shake table investigation on interaction between buildings in a row, Coupled Systems Mechanics Vol 2, No 2, pp 175-90.

Li, B., Bi, K., Chouw, N., Butterworth, J.W., and Hao, H. (2012) Experimental investigation of spatially varying effect of ground motions on bridge pounding, Earthquake Eng Struct Dyn Vol 41, No 14, pp 1959-76.

Li, B., Bi, K., Chouw, N., Butterworth, J.W. and Hao, H. (2013) Effect of abutment excitation on bridge pounding, Eng Struct Vol 54, pp 57-68.

Mahmoud, S. (2008). Modified linear viscoelastic model for elimination of the tension force in the linear viscoelastic, Proc. of the 14th World Conf. on Earthquake Engineering, Beijing, China.

Malhotra, P. (1998) Dynamics of seismic pounding at expansion joints of concrete bridges, ASCE J Eng Mech Vol 124, No 7, pp 794-802.

Muthukumar, S. and DesRoches, R. (2006) A hertz contact model with non linear damping for pounding simulation, Earthquake Eng Struct Dyn Vol 35, No 7, pp 811-28.

Rosenblueth, E. and Meli, R. (1986) The 1985 earthquake: Causes and effects in mexico city, Concr Int Vol 8, No 5, pp 23-34.

Schmid, G. and Chouw, N. (1992). Soil-structure interaction effects on structural pounding, Proc. of the 10 World Conf. on Earthquake Engineering, Balkema, Rotterdam, 1651-6.

Ye, K., Li, L. and Zhu, H. (2009a) A modified kelvin impact model for pounding simulation of base-isolated building with adjacent structures, Earthquake Eng and Eng Vibration Vol 8, No 3, pp 433-46.

Ye, K., Li, L. and Zhu, H. (2009b) A note on the hertz contact model with nonlinear damping for pounding simulation, Earthquake Eng Struct Dyn Vol 38, No 9, pp 1135-42.

Zhang, Y. and Sharf, I. (2009) Validation of nonlinear viscoelastic contact force models for low speed impact, J Appl Mech Vol 76, pp 051002.